NeuroImage **10,** 173–180 (1999)
Article ID nimg.1999.0454, available online at http://www.idealibrary.com on IDEAL®

Visualization of Magnetoencephalographic Data Using Minimum Current Estimates

K. Uutela,* M. Hämäläinen,* and E. Somersalo†

**Brain Research Unit, Low Temperature Laboratory, and †Institute of Mathematics, Helsinki University of Technology, FIN-02015 HUT Espoo, Finland*

Received December 1, 1998

The locations of active brain areas can be estimated from the magnetic field the neural current sources produce. In this work we study a visualization method of magnetoencephalographic data that is based on minimum ℓ^1-norm estimates. The method can represent several local or distributed sources and does not need explicit *a priori* information. We evaluated the performance of the method using simulation studies. In a situation resembling typical magnetoencephalographic measurement, the mean estimated source strength exceeded baseline level up to 2 cm from the simulated point-like source. The method can also visualize several sources, activated simultaneously or in a sequence, which we demonstrated by analyzing magnetic responses associated with sensory stimulation and a picture naming task.

INTRODUCTION

Magnetoencephalography (MEG) (Hämäläinen *et al.*, 1993) is a functional brain imaging method with an excellent temporal resolution. However, the source locations can be obtained from MEG data unambiguously only if suitable constraints are imposed. Therefore, it has been difficult to interpret the data and to combine MEG with other functional imaging methods.

In this article we present an MEG visualization method that can be used without explicit *a priori* information and can represent several local or distributed sources, even when they overlap in time.

Using parametric dipole models (Brenner *et al.*, 1978; Tuomisto *et al.*, 1983; Scherg, 1990; Mosher *et al.*, 1992; Uutela *et al.*, 1998) the active brain areas can be located with an accuracy of about 0.5 cm if the model structure, i.e., the number of active sources and their time spans, is correct. However, it is not straightforward to select an appropriate model when several temporally overlapping sources are active. Some objective methods for model structure selection have been proposed, but currently the most practical approach is that an experienced scientist generates the models by trial and error.

The minimum current estimate (MCE) belongs to the class of minimum norm estimates (Hämäläinen and Ilmoniemi, 1994; Ioannides *et al.*, 1990; Dale and Sereno, 1993; Pascual-Marqui *et al.*, 1994; Matsuura and Okabe, 1995). These estimates do not impose explicit constraints on the current distribution but, instead, select the most plausible source distribution among the ones compatible with the measurements. The results are usually blurred because of the relatively long distance from the sensors to the sources and the noise in the recorded signals. Still, the estimates may assist a scientist visualizing the data and selecting a good model structure for multidipole models.

METHODS

General Minimum Norm Estimate

The MEG signals at a given time point can be modeled using a discrete linear model (Hämäläinen *et al.*, 1993)

$$\mathbf{b} = \mathbf{G}\,\mathbf{q} + \mathbf{n}, \tag{1}$$

where $\mathbf{b}$ is a vector of the measured signals, $\mathbf{G}$ is a gain matrix consisting of the magnetic signals produced by unit sources at different locations and orientations, $\mathbf{q}$ is a vector consisting of the source strengths, and $\mathbf{n}$ is a noise vector.

Although the measured data $\mathbf{b}$ do not give the source strengths $\mathbf{q}$ unambiguously if the number of discretized sources is larger than the number of sensors, a minimum norm estimate of $\mathbf{q}$ can be calculated as a solution of the optimization problem

$$\min \|\mathbf{q}\| \tag{2}$$

subject to

$$\mathbf{G}\,\mathbf{q} \approx \mathbf{b}. \tag{3}$$

1053-8119/99 $30.00

This approach has different forms depending on how the norm is selected in Eq. (2) and what kind of errors are tolerated in Eq. (3) (the selection of the regularization method).

Regularization

The estimation of the current distribution on the basis of the measured magnetic fields is an ill-posed problem: small variations in the measured signals may change the estimated current distributions considerably. However, the variance of the estimated current density can be reduced by allowing a slight bias: the estimate is regularized. The regularization can be viewed as incorporating prior information to the estimation problem. The most commonly used regularization methods are the Tikhonov or Wiener regularization (Tikhonov and Arsenin, 1977; Foster, 1961) and the singular value decomposition method, which is employed in MCE.

Let $\mathbf{G} = \mathbf{U}\mathbf{\Lambda}\mathbf{V}^{\mathrm{T}}$ be the singular value decomposition of the gain matrix $\mathbf{G}$. Here, $\mathbf{U}$ and $\mathbf{V}$ are unitary matrices and $\mathbf{\Lambda}$ is a diagonal matrix, the diagonal elements being the singular values in decreasing order. With cutoff index n, the regularized version of the optimization problems (2) and (3) assumes the form

$$\min \|\mathbf{q}\| \tag{4}$$

subject to the constraint

$$\mathbf{\Lambda}_n \mathbf{V}^{\mathrm{T}} \mathbf{q} = \mathbf{U}_n^{\mathrm{T}} \mathbf{b}, \tag{5}$$

where $\mathbf{\Lambda}_n$ includes the n rows of $\mathbf{\Lambda}$ (i.e., n largest singular values) and $\mathbf{U}_n$ includes the n first columns of $\mathbf{U}$. The optimal value for the regularization parameter n depends on the signal-to-noise ratio of the measurements: The smaller n is, the greater the allowed mismatch between $\mathbf{b}$ and $\mathbf{G}\mathbf{q}$ can be while still satisfying constraint (5).

Minimum Current Estimate

The minimum current estimate minimizes the sum of the absolute currents (ℓ^1-norm) (Matsuura and Okabe, 1995). This leads to more focal source estimates than estimates using Euclidean (ℓ^2) norm and can represent well the relatively compact source areas typically activated in the sensory projection areas. Norms with orders between 1 and 2 could be used for estimates with properties between the ℓ^1- and ℓ^2-norms (Beucker and Schlitt, 1996), but iterative methods would be needed to calculate them.

In Bayesian sense, the minimum ℓ^2-norm estimate can be thought of as the maximum *a posteriori* probability estimate with Gaussian *a priori* current distribution, while the minimum ℓ^1-norm estimate corresponds to an exponential *a priori* distribution (Fig. 1).

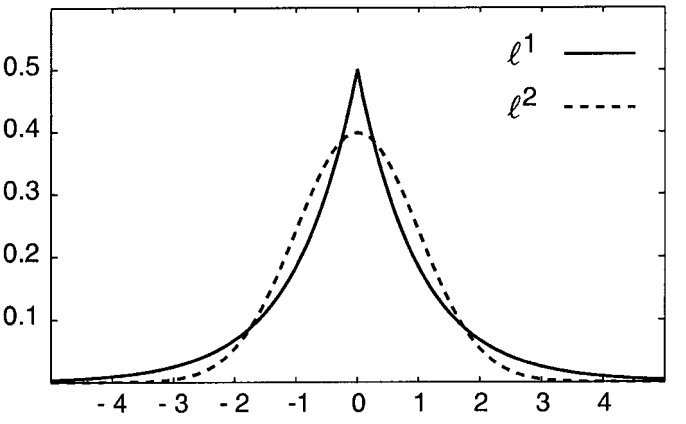

FIG. 1. *A priori* distributions of current amplitudes in minimum ℓ^1- and ℓ^2-norm estimates.

The magnetic field produced by a deep focal source can be very similar to that of a superficial, extended source. Because measurements are more sensitive to the superficial sources, the ordinary minimum norm estimate has a bias toward these. This bias can be compensated by using a weighted norm (Ioannides *et al.*, 1990; Köhler *et al.*, 1996) where the weight of each source component in vector $\mathbf{q}$ of Eq. (2) is proportional to the strength of the signal that a constant current in the same location produces, i.e., the Euclidean norm of a row of matrix $\mathbf{G}$. The weighted ℓ^1-norm of $\mathbf{q}$ is

$$\|\mathbf{q}\|_{1,w} = \sum_{j=1}^{N} w_j \|\mathbf{q}_j\|_2, \tag{6}$$

where w_j and $\mathbf{q}_j$ are weight and current vector at source location j and N is the number of different source locations.

The drawback of the minimum ℓ^1-norm estimate, compared with minimum ℓ^2-norm estimate, is that the optimization problem cannot be solved directly. However, linear programming (LP) solves the problem efficiently, if the current orientations can be assumed to be known in advance. Because of the columnar organization of the cortex, the observable sources are typically perpendicular to the cortical surface. Magnetic resonance (MR) images can be used to determine the normal of the cortex at given points and thus also the most probable current orientation (Dale and Sereno, 1993). Since the cortex is heavily convoluted, a large number of points are required to represent its geometry accurately. However, the use of a dense point set may be unnecessary because of the relatively poor spatial resolution of MEG. Using an excessive number of reconstruction points also increases the computational burden in the calculation of the ℓ^1-norm estimate.

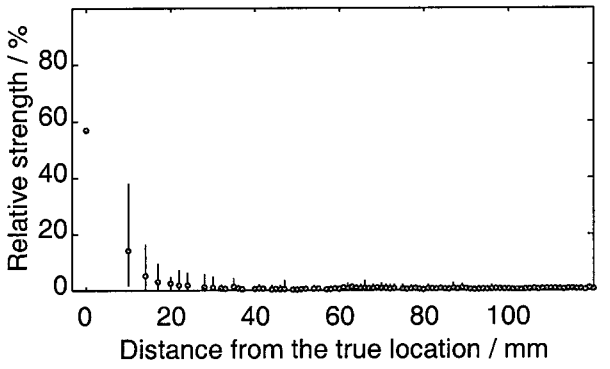

FIG. 2. Average source strength as percentage of the strength of the simulated source. The circles show the mean values and the lines the 5 and 95% percentiles.

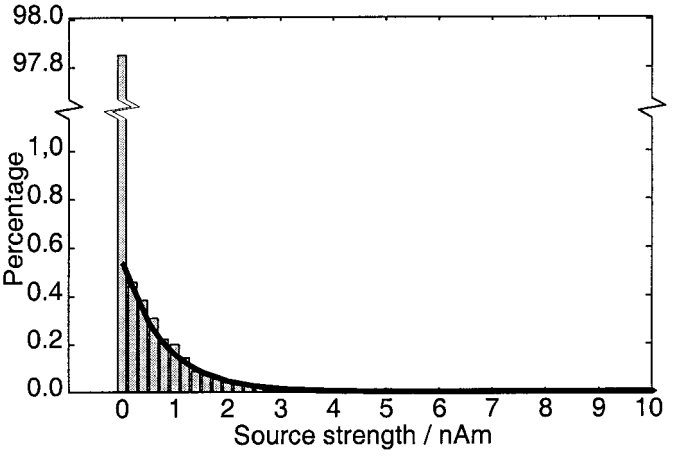

FIG. 3. The distribution of current amplitudes estimated from simulated noise (gray bars). The solid line shows the exponential distribution fitted to the nonzero values.

Therefore, we used a sparser point set and selected the current orientations with help of the minimum ℓ^2-norm solution. The LP algorithm can also be modified to iteratively update the orientations (Matsuura and Okabe, 1996), but the results do not seem to be significantly better, partly because of convergence problems.

The cutoff index n is also the number of constraints in the LP problem; thus the maximum number of source locations having nonzero current at any single time point is n.

The algorithm consists of the following steps:

1. Find the minimum weighted ℓ^2-norm estimate $\mathbf{q}_0$ by minimizing

$$\sum_{j=1}^{N} w_j^2 \, \|\mathbf{q}_j\|_2^2$$

subject to the constraint

$$\mathbf{\Lambda}_n \mathbf{V}^{\mathrm{T}} \mathbf{q} = \mathbf{U}_n^{\mathrm{T}} \mathbf{b}.$$

2. Create the orientation matrix $\mathbf{\Theta}$ in which each row is a vector describing the current orientation in $\mathbf{q}_0$ in the corresponding location. Scale the vectors to Euclidean norm one.

3. Find the weighted minimum ℓ^1-norm estimate by minimizing

$$\sum_{j=1}^{N} w_j t_j$$

with respect to source strength vector $\mathbf{t}$ subject to the constraints

$$\mathbf{\Lambda}_n \mathbf{V}^{\mathrm{T}} \mathbf{\Theta} t = \mathbf{U}_n^{\mathrm{T}} \mathbf{b}, \quad t_j \geq 0.$$

Visualization

To visualize the three-dimensional estimates they are shown on a triangle mesh representing the surface of the brain (Fig. 5). The neural currents are estimated in points of a three-dimensional cubical lattice within the brain. The estimated current of each location is projected along a radius from the origin of the spherically symmetric head model employed in the calculations. The current strength is weighted inversely proportionally to the distance from the projected location to the vertices of the triangle and added to the activity at the vertices. Thus estimated currents from locations directly under a node on the surface is shown almost totally in that node, and the estimated current from a location between adjacent nodes is reflected in all of them. The results are shown with interpolated color coding on the triangle net.

The program calculating and visualizing the estimates was implemented using Matlab. The LP problem was solved using the lp_solve library by Michel Berkelaar. After the initialization, the calculation typically took 1–2 s/time point in an HP C160 workstation.

FIG. 4. The source distributions (color coded) estimated from simulated source distributions (green arrows): (a) a single focal source, (b) an active patch of cortex, (c) two parallel focal sources, and (d) two orthogonal focal sources.

FIG. 5. MCE of somatosensory evoked fields 15–40 ms (a) and 100–150 ms (b) after the stimulus. Corresponding multidipole model projected on subject's MR images (c).

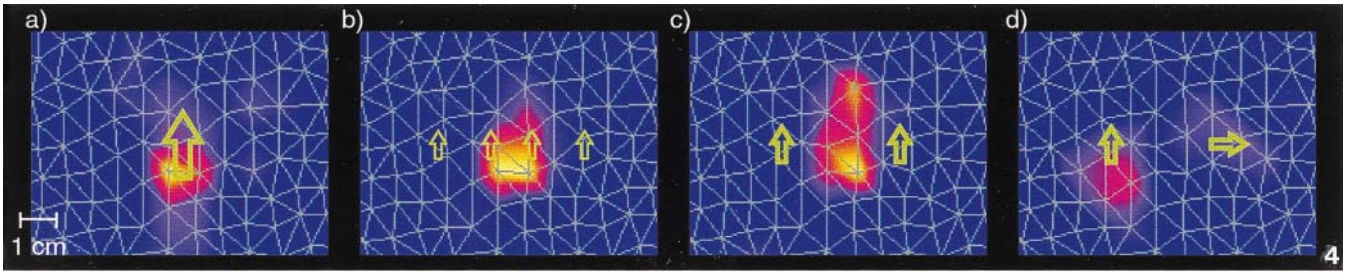
a)
b)
c)
d)
1 cm
4

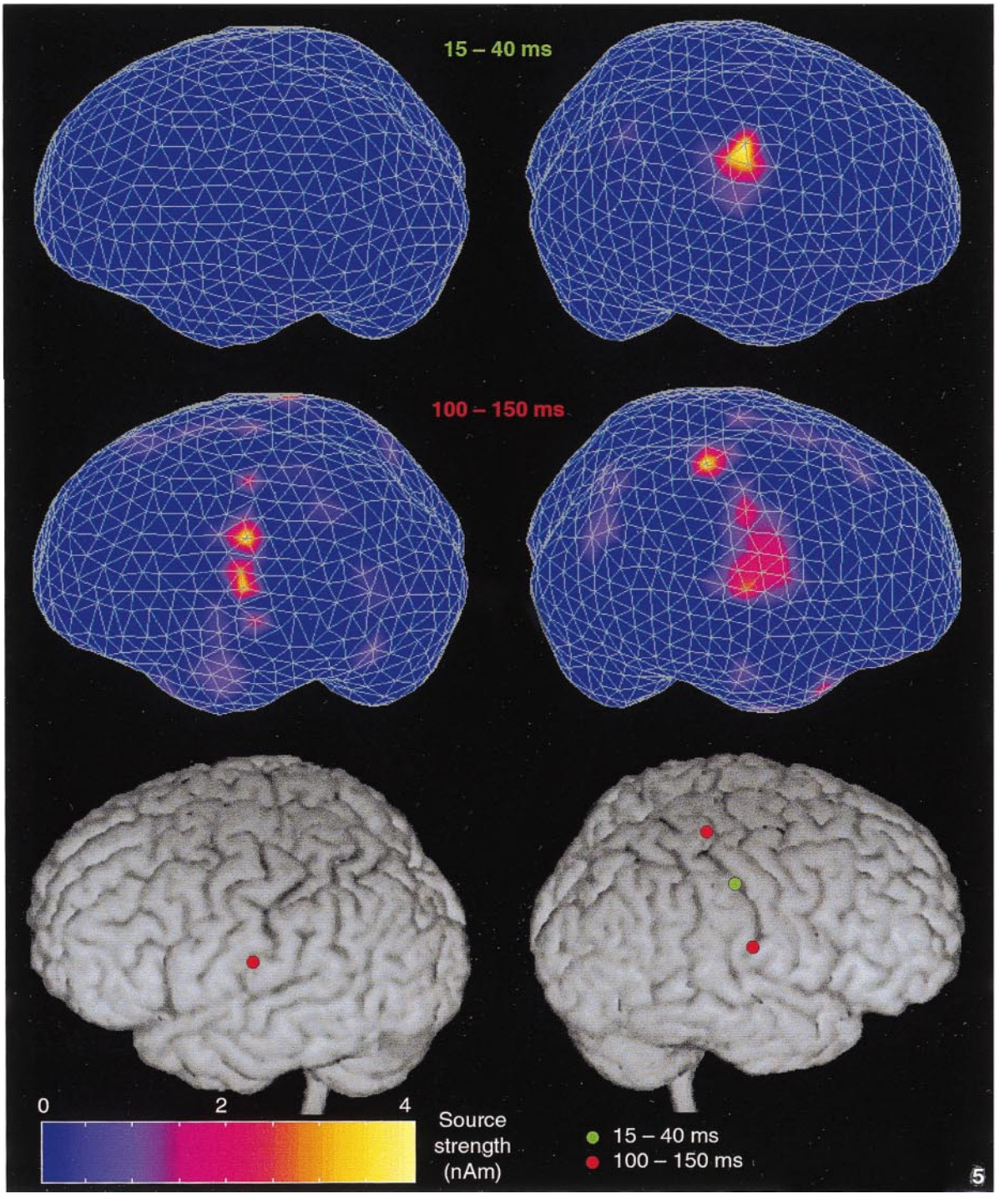
15 – 40 ms
100 – 150 ms
0
2
4
Source strength (nAm)
15 – 40 ms
100 – 150 ms
5

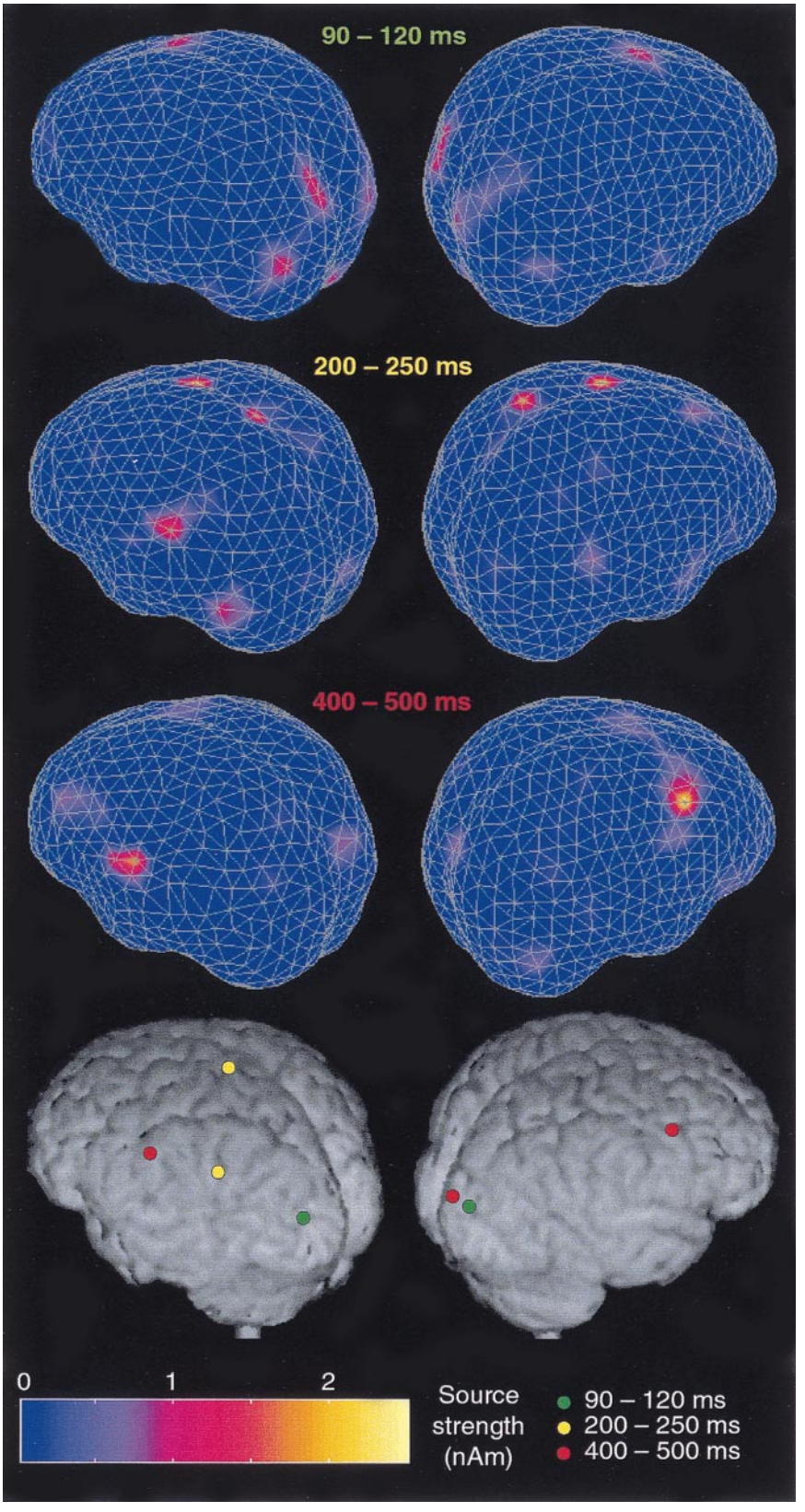

FIG. 6. MCE of fields evoked by picture naming using time span 90–160 ms (a), 200–250 ms (b), and 400–500 ms (c) after stimulus and dipole modeling results projected on subject's MR images (d).

SIMULATIONS

Signals measured with a Neuromag-122 system (Ahonen *et al.*, 1993) were simulated to evaluate the performance of the method. The magnetic field generated by a single current dipole was calculated using a single-compartment boundary-element conductor model assuming the shape of the cranial volume. In MCE, spherically symmetric conductor model was used; thus the estimation included modeling errors in the forward problem, which cannot be avoided in real measurements.

Simulated noise whose spatial and temporal correlations resembled that of the real measurements, including spontaneous background activity of the brain, was added: The spatial distribution of the noise was a combination of signal arising from random dipoles within the head (de Munck *et al.*, 1992) and white noise. The temporal noise characteristics were simulated using an autoregressive model of measured background activity. A 50-Hz noise component was also added. The noise corresponded to 10% of the variance of the simulated data.

The MCE was calculated from this simulation; the cutoff index of regularization was 30. The possible source locations were constrained to the brain volume in a simple cubical lattice with lattice constant of 10 mm. Locations closer than 30 mm to the center of the sphere model were excluded, because currents in these areas produce very weak magnetic signals. Figure 2 shows the estimated source strength as a function of the distance from the true source location.

Noise and modeling errors spread the main peak in the estimation results to some extent. The amplitude of the estimated current at the closest node was 57% of the correct value. The rest of the current had spread to the nearby nodes: the estimated current strength exceeded the baseline variations in nodes up to 20 mm from the simulated source.

The distribution of the noise of the estimate was studied by calculating MCE from a simulation of noise in an evoked response measurement with 100 averages. The noise level was 8 fT/cm, and the spatial and temporal characteristics were the same as in the previous simulation.

Because of the regularization, 98% of the estimated currents were zeros. The nonzero values were approximately exponentially distributed with mean value of 0.8 nAm (Fig. 3).

Because there is no one-to-one relationship between current distributions and measured magnetic fields, there are equivalent source distributions that cannot be discriminated by MEG recordings. For example, a small extended source, a few focal sources next to each other with parallel currents, and a single dipole each produce very similar magnetic fields. The separability of two focal sources depends on the angle between the currents; magnetic fields produced by sources with perpendicular currents cannot be explained well with a single source (Lütkenhöner, 1998).

To demonstrate the situation, we calculated the magnetic fields, as measured with a Neuromag-122, of four current distributions: a single current dipole, a 5-cm-wide patch with constant current, and two dipoles with a 3-cm distance with parallel and orthogonal currents. The distance from the center of the sphere model to the extended currents was 6 cm, and to the single source 4.5 cm. The correlation coefficients between two of the first three cases were 0.97–0.98, and the data vectors corresponding to any coefficients between the perpendicular source case and the others were 0.56–0.57.

As in the previous simulations, noise amounting to 10% of the variance of the simulated data was added. For each source configuration the current distribution was estimated over a 30-ms time period. Because MCE favors focal sources, the estimates current of the patch and the two dipoles with parallel currents concentrated around the location of the single source (Figs. 4a–4c), whereas the orthogonal currents produced two distinct clusters (Fig. 4d).

The resolution of the method depends basically on the ability to measure the differences between the source distributions and in a general case cannot be drastically improved. However, there is some *a priori* information that can be incorporated. In MEG measurements, the same sources are active during several time points, and unless their time courses are too similar, their relative strength varies. This leads to estimates where the strongest currents overlap the real sources at some time points and a focal current seems to move between them, when the source strengths are balanced. The temporal information could be automatically incorporated to the estimate, for example, by using MUSIC algorithm (Mosher *et al.*, 1992) to assign weights to different source locations (Dale and Sereno, 1993). Also, if functional MR data of a similar measurement are available, the result can be used to enhance the spatial resolution (Dale *et al.*, 1997; Uutela and Ryymin, 1998).

MEASURED DATA

Somatosensory Evoked Fields

To assess the performance of the method with real MEG data we calculated the MCE from magnetic responses evoked by somatosensory stimuli. Median nerve stimulation activates several brain areas with temporal overlap. Because the somatosensory responses have been studied extensively (Brenner *et al.*, 1978; Hari *et al.*, 1984; Forss *et al.*, 1994), the areas producing the main activations are known: The primary somatosensory cortex (S1) contralateral to the stimulus is activated beginning approximately 20 ms

after the stimulus. Later, typically around 100–140 ms, the secondary somatosensory cortices are activated bilaterally. Activity of the contralateral posterior parietal cortex is also often seen (Forss *et al.*, 1994).

Schnitzler *et al.* (1995) stimulated electrically the left median nerve of the subject once every 1.5 s and measured the evoked responses with Neuromag-122. The signal was analogically low-pass filtered at 330 Hz, sampled at 1 kHz, low-pass filtered offline with cutoff frequency 90 Hz, and decimated to 250 Hz.

The MCE was calculated from these data with 30 singular values (Fig. 5). The estimate shows a clear source in the hand area of the S1 15–20 ms after the stimulation. Later, during time range 100–150 ms, the secondary somatosensory cortices and the parietal cortex are active. The widespread weak activity seen in the estimate between 100 and 150 ms may reflect larger spatial extent of the activated areas at the later stages of sensory processing or possibly recruitment of some additional areas. According to the simulation studies, the strongest source areas should be correctly located; the locations of the strongly activated areas are also concordant with a multidipole model of the same data.

Naming Task

To assess the performance of the method with a more complex source distribution we calculated the MCE from magnetic responses associated with a picture naming task. The exact cortical sites involved in language processing vary between subjects, but typically during the first 200 ms after picture onset the visual areas of the occipital lobe are active. During the next 200 ms the posterior language area near the left temporoparietooccipital junction is activated and subsequently the frontal language and mouth motor areas; the corresponding areas in the right hemisphere are often active as well (Ojemann, 1990; Salmelin *et al.*, 1994).

Levelt *et al.* (1998) presented black and white line drawings of familiar objects to a healthy subject, who named them aloud as quickly as possible. The evoked fields were measured using Neuromag-122 and averaged with respect to picture onset. The averages were low-pass filtered with a cutoff frequency of 40 Hz.

The MCE was calculated from these data using 30 singular values (Fig. 6). The magnetic field at 100 ms after picture onset yielded an estimate with activity mainly in the occipital areas. Later, between 200 and 250 ms, the parietal cortex near the midline and an area near the end of the Sylvian fissure were most strongly activated. Between 400 and 500 ms, areas near the junction of central sulcus and Sylvian fissure were strongly activated. The results resemble the source locations obtained using automatic multidipole modeling of the same data (Uutela *et al.*, 1998).

CONCLUSIONS

The MCE shows good performance both with simulated data and with real MEG measurements. Unlike the minimum ℓ^2-norm estimate, the estimate is close to the actual distribution when the true sources are focal. No assumptions about the activation sequence are made, and the time course of each source can also be estimated.

The accuracy of MCE is not as good as that of a dipole model for a single source, but because MCE needs minimal user intervention, it is objective and easy to calculate and not prone to modeling errors.

MCE is useful for visualizing the sources of MEG signals and for selecting the model structure for multidipole analysis. Because the MCE is a three-dimensional estimate of the brain activity, the method is also suitable for combined analysis of MEG and other imaging modalities.

ACKNOWLEDGMENTS

The authors thank Schnitzler *et al.* and Levelt *et al.* for the measured data used in the examples and Mika Seppä for help in work with MR images. Supported by the Ministry of Education.

REFERENCES

Ahonen, A. I., Hämäläinen, M. S., Kajola, M. J., Knuutila, J. E. T., Laine, P. P., Lounasmaa, O. V., Parkkonen, L. T., Simola, J. T., and Tesche, C. D. 1993. A 122-channel SQUID instrument for investigating the magnetic signals from the human brain. *Phys. Scripta* **T49:** 198–205.

Beucker, R., and Schlitt, H. A. 1996. On minimal ℓ_p-norm solutions of the biomagnetic inverse problem. *IEEE Trans. Biomed. Eng.*, submitted for publication.

Brenner, D., Lipton, J., Kaufman, L., and Williamson, S. J. 1978. Somatically evoked magnetic fields of the human brain. *Science* **199:** 81–83.

Dale, A., Halgren, E., and Lewine, J. 1997. Spatio-temporal localization of cortical word repetition effects in a size judgment task using combined fMRI/MEG. *NeuroImage* **5:** S592.

Dale, A., and Sereno, M. 1993. Improved localization of cortical activity by combining EEG and MEG with MRI cortical surface reconstruction: A linear approach. *J. Cogn. Neurosci.* **5:** 162–176.

de Munck, J. C., Vijn, P. C. M., and Lopes da Silva, F. H. 1992. A random dipole model for spontaneous brain activity. *IEEE Trans. Biomed. Eng.* **39:** 791–804.

Forss, N., Hari, R., Salmelin, R., Ahonen, A. I., Hämäläinen, M. S., Kajola, M. J., Knuutila, J. E. T., and Simola, J. T. 1994. Activation of the human posterior parietal cortex by median nerve stimulation. *Exp. Brain Res.* **99:** 309–315.

Foster, M. 1961. An application of the Wiener-Kolmogorov smoothing theory to matrix inversion. *J. Soc. Indust. Appl. Math* **9:** 387–392.

Hämäläinen, M., Hari, R., Ilmoniemi, R. J., Knuutila, J., and Lounasmaa, O. V. 1993. Magnetoencephalography—Theory, instrumentation, and applications to noninvasive studies of the working human brain. *Rev. Mod. Phys.* **65:** 413–497.

Hämäläinen, M. S., and Ilmoniemi, R. J. 1994. Interpreting magnetic fields of the brain: Minimum norm estimates. *Med. Biol. Eng. Comput.* **32:** 35–42.

Hari, R., Reinikainen, K., Kaukoranta, E., Hämäläinen, M., Ilmoniemi, R., Penttinen, A., Salminen, J., and Teszner, D. 1984. Somatosensory evoked cerebral magnetic fields from SI and SII in man. *Electroenceph. Clin. Neurophysiol.* **57:** 254–263.

Ioannides, A., Bolton, J., and Clarke, C. 1990. Continuous probabilistic solutions to the biomagnetic inverse problem. *Inverse Problems* **6:** 523–542.

Köhler, T., Wagner, M., Fuchs, M., Wischmann, H.-A., Drenkhahn, R., and Theißen, A. 1996. Depth normalization in MEG/EEG current density imaging. In *Conference Proceedings of the 18th Annual International Conference of the Engineering in Medicine and Biology Society of the IEEE*, Amsterdam.

Levelt, W. J. M., Praamstra, P., Meyer, A. S., Helenius, P., and Salmelin, R. 1998. An MEG study of picture naming. *J. Cogn. Neurosci.* **10:** 553–567.

Lütkenhöner, B. 1998. Dipole separability in a neuromagnetic source analysis. *IEEE Trans. Biomed. Eng.* **45:** 572–581.

Matsuura, K., and Okabe, U. 1995. Selective minimum-norm solution of the biomagnetic inverse problem. *IEEE Trans. Biomed. Eng.* **42:** 608–615.

Matsuura, K., and Okabe, Y. 1999. Multiple current-dipole distribution reconstructed by modified selective minimum-norm method. In *Advances in Biomagnetism Research: Biomag96* (C. Aine, Y. Okada, G. Stroink, S. Swithenby, and C. Wood, Eds.), in press. Springer-Verlag, Berlin.

Mosher, J. C., Lewis, P. S., and Leahy, R. M. 1992. Multiple dipole modeling and localization from spatio-temporal MEG data. *IEEE Trans. Biomed. Eng.* **39:** 541–557.

Ojemann, G. A. 1990. Organization of language cortex derived from investigations during neurosurgery. *Semin. Neurosci.* **2:** 297–305.

Pascual-Marqui, R. D., Michel, C. M., and Lehmann, D. 1994. Low-resolution electromagnetic tomography: A new method for localizing electrical activity in the brain. *Int. J. Psychophysiol.* **18:** 49–65.

Salmelin, R., Hari, R., Lounasmaa, O. V., and Sams, M. 1994. Dynamics of brain activation during picture naming. *Nature* **368:** 463–465.

Scherg, M. 1990. Fundamentals of dipole source potential analysis. In *Advances in Audiology.* Vol 6. *Auditory Evoked Magnetic Fields and Electric Potentials* (F. Grandori, M. Hoke, and G. L. Romani, Eds.), pp. 40–69. Karger, Basel.

Schnitzler, A., Salmelin, R., Salenius, S., Jousmäki, V., and Hari, R. 1995. Tactile information from the human hand reaches the ipsilateral primary sensory cortex. *Neurosci. Lett.* **200:** 25–28.

Tikhonov, A. N., and Arsenin, V. Y. 1977. *Solutions of Ill-Posed Problems,* Scripta Series in Mathematics. Wiley, New York.

Tuomisto, T., Hari, R., Katila, T., Poutanen, T., and Varpula, T. 1983. Studies of auditory evoked magnetic and electric responses: Modality specificity and modelling. *Il Nuovo Cimento* **2D:** 471–483.

Uutela, K., Hämäläinen, M., and Salmelin, R. 1998. Global optimization in the localization of neuromagnetic sources. *IEEE Trans. Biomed. Eng.* **45:** 716–723.

Uutela, K., and Ryymin, P. 1998. Combined analysis of MEG and fMRI using minimum ℓ^1-norm estimates. In *Proceedings of the 11th International Conference on Biomagnetism* (H. Karibe, Ed.), in press. Sendai, Japan.